Mechanism of Heat Transfer to Fluidized Beds

H. S. Mickley and D. F. Fairbanks

Massachusetts Institute of Technology, Cambridge, Massachusetts

In order to determine the nature of the resistance controlling heat transfer between fluidized beds and surfaces in contact with them, heat transfer measurements were made on the same solid constituents with several different fluidizing gases. The heat transfer coefficients obtained with fluidized beds are found to be proportional to the square root of the thermal conductivity of the quiescent beds. This result indicates that the process controlling fluidized heat transfer may be considered to be an unsteady-state diffusion of heat into mobile elements of quiescent bed material.

This picture is analyzed mathematically to yield an equation for the heat transfer coefficient $h = \sqrt{\kappa_m \rho_m c S}$ wherein the effects of the bed thermal properties are separated from the effects of the stirring factor S, which accounts for bed motion and geometry. The mass transfer analogue is also derived and shown to correlate existing mass and heat transfer data reasonably well.

It is concluded that the proposed mechanism yields a satisfactory picture of the fluidized heat transfer process and may provide the beginnings of a rational approach to the correlation and prediction of fluidized heat transfer in engineering work.

Heat transfer coefficients of up to 300 B.t.u./(hr.)(sq.ft.)(°F.) have been reported(*8*) for fluidized beds and surfaces in contact with them; values in the range of 40 to 120 B.t.u./(hr.)(sq.ft.)(°F.) are common. Such coefficients are many times higher than those normally encountered with packed beds or with flowing gases, and the resulting ease of heat transfer is one of the factors favoring the incorporation of fluidization into industrial processes. Despite the many successful commercial applications of fluidization, the nature of the heat-transfer process has remained obscure. The present investigation represents an attempt to delineate the mechanism of heat transfer in "bubbling" beds, i.e., dense-phase, aggregative beds in the absence of slugging or severe channeling. Such beds are a type commonly desired for industrial applications and may be qualitatively described as inhomogeneous tumbling mixtures of solids and upward-moving gas-filled spaces. Knowledge of the heat-transfer mechanism should be of considerable aid in the development of trustworthy design procedures for these beds.

DEVELOPMENT OF A MODEL

As a first step in developing a picture of the mechanism of fluidized heat transfer, it is to be noted that at any time in a fluidized system which is in contact with a surface hotter or colder than the bed, transitory solid-solid, solid-surface, gas-solid, and gas-surface contacts are all occurring, with interconduction of heat to be expected from each such contact. The complicated, irregular motions of solids and gas are constantly making and destroying the individual contacts, and these motions create the means for a convective transfer of heat via both media. By the simultaneous and successive operations of all these individual conductive and convective mechanisms, heat is transferred from the surface and into the core of the bed.

The difficulty with this mode of depicting the heat transfer process is that while the picture is almost certainly correct, it is so complicated as to be quantitatively unmanageable. The need for the creation of a manageable model is the justification for the following discussion.

Bauer(*2*) found evidence that the dense phase of bubbling beds retained a constant void fraction independent of superficial gas velocity and that this void fraction was essentially that of quiescence. Furthermore, his data for uniform glass spheres indicate that the void fraction of quiescence was 0.41. This value may be compared with the theoretical void fractions for spheres packed in cubic and hexagonal prism lattices: 0.475 and 0.395, respectively. In these two

theoretical lattice structures there are, respectively, six and eight neighbors in direct contact with each sphere. It may be concluded, therefore, that at least for uniform spheres the quiescent packing is close enough to allow each particle to be in direct contact with nearly eight neighbors. Each particle in the dense phase of a fluidized bed may be expected to be in contact with several neighbors most of the time, and with this the case it does not seem unreasonable to assume that the particles are locked loosely together and do not usually move in relation to one another. Of course, if the motion of the bed

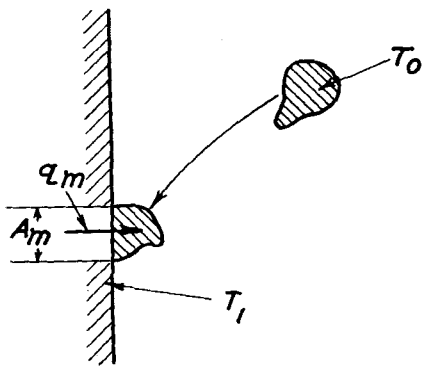

Fig. 1. Transfer of a packet to a heated surface.

creates localized temporary shear forces, separation or relative motion of neighboring particles will result. However, if a small group of *neighboring* particles is considered, it would appear that it will be a fairly rare occurrence for this group to be so ruptured. It seems reasonable, therefore, to create a picture of fluidization in which small groups of particles are imagined to move as individual units through the bed as the dense phase is stirred. Such a small group or assembly of particles will be here termed a *packet*. Packets are not permanent, but they may be accorded some finite persistence in time. Their void fraction, density, and heat capacity are those of the quiescent bed. The packet thermal conductivity is that of the bed when measured at quiescent packing density in the absence of any solid motion.

In Figure 1 a packet is represented in the main body of the bed. It is here at bed temperature T_o. Suppose that the stirring of the dense phase sweeps this particular packet into contact with a flat surface of temperature T_1. Unsteady-state diffusion of heat into the packet will commence upon contact, and, if it is assumed for analytical purposes that the packet may be considered homogeneous, it can be shown(4) that after being in contact for a time τ, the rate of diffusion of heat into the packet is

$$q_m = \frac{A_m}{\sqrt{\pi}} \sqrt{\kappa_m \rho_m c}\, \tau^{-1/2} (T_1 - T_o) \tag{1}$$

where

q_m is the instantaneous rate of heat flow into the packet, B.t.u./hr.

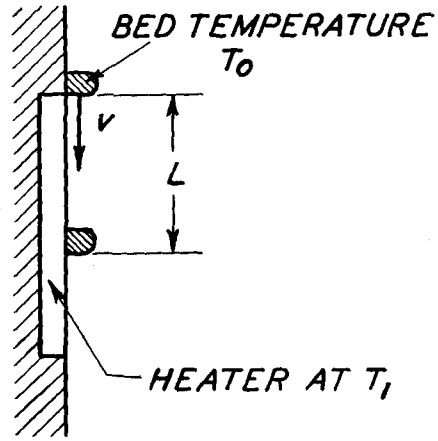

Fig. 2. Downflow of packets past a heated surface.

A_m is the area of contact of the packet with the surface, sq.ft.

κ_m is the thermal conductivity of the packet B.t.u./(hr.)(ft.)(°F.)

ρ_m is the density of the packet, lb./cu.ft.

c is the heat capacity of the packet, B.t.u./(lb.)(°F.)

If the local instantaneous heat transfer coefficient is represented by h_i, then

$$h_i = \frac{q_m}{A_m (T_1 - T_o)} = \frac{1}{\sqrt{\pi}} \sqrt{\kappa_m \rho_m c}\, \tau^{-1/2} \tag{2}$$

The observed local heat transfer coefficient will be the time average of all the local, instantaneous coefficients occurring during a period of time at a particular locality on the heater surface. At this location, let $\psi(\tau)$ represent the frequency of occurrence in time of packets having age τ; that is, over a long period of time, the fraction of the total time during which the surface is in contact with packets of ages ranging between τ and $\tau + d\tau$ is $\psi(\tau)d\tau$. The observed local average coefficient will be due to heat transfer to packets of all ages plus that due to direct contact of gas bubbles at the surface. Neglecting the latter effect, which should generally be small, results in the local coefficient expressed mathematically as the summation of the individual contributions of packets of all ages:

$$h_L = \int_o^\infty h_i(\tau)\, \psi(\tau)\, d\tau = \frac{1}{\sqrt{\pi}} \sqrt{\kappa_m \rho_m c} \int_o^\infty \tau^{-1/2} \psi(\tau)\, d\tau \tag{3}$$

If the term S_L is defined as

$$S_L = \frac{1}{\pi} \left[\int_o^\infty \tau^{-1/2} \psi(\tau)\, d\tau \right]^2 \tag{4}$$

Equation (3) may be succinctly written as

$$h_L = \sqrt{\kappa_m \rho_m c\, S_L} \tag{5}$$

Two important assumptions have entered into this derivation, viz., (1) that relative motion of neighboring particles is rare, at least near heater surfaces, and (2) that the dense phase of the fluidized bed may for the present purpose be considered homogeneous. Some justification has already been given for the first assumption. The second assumption will probably be good if the average residence time of the solid in contact with the surface is long enough for a fair portion of the heat transferred to diffuse into layers of particles lying beyond the layer touching the surface. Justification of the latter assumption requires experimental evidence, which will be offered at a later point.

AVERAGE COEFFICIENTS

Generally one is more interested in the average coefficient for an entire surface than in the local coefficient at a particular point on that surface. The average coefficient for an isothermal surface will be the area mean of the local coefficients. Thus,

$$h = \frac{1}{A} \int_A h_L\, dA \tag{6}$$

where A represents the area of the heat transfer surface. Combining Equations (5) and (6) gives

$$h = \frac{1}{A}\sqrt{\kappa_m \rho_m c}\int_A S_L^{1/2}\,dA \quad (7)$$

By defining an area mean stirring factor S as

$$S^{1/2} = \frac{1}{A}\int_A S_L^{1/2}\,dA \quad (8)$$

one may write the mean coefficient in a form analogous to Equation (5),

$$h = \sqrt{\kappa_m \rho_m c S} \quad (9)$$

VALUE OF THE MODEL

If Equations (3) and (5) are examined, it will be noted that they relate the heat transfer coefficient to the product of two terms. One of these terms, $\sqrt{\kappa_m \rho_m c}$, is a function only of the thermal properties of the quiescent bed and is readily evaluated. The other term, S_L, offers more difficulty, for it is a function of the packet-age distribution, $\psi(\tau)$, and little is known about how this distribution may be affected by the gross operating variables of the system: gas velocity, particle diameter, heater size, etc. The relation between the two terms S_L and $\psi(\tau)$ is as follows. If solid is exchanged very rapidly at the surface, $\psi(\tau)$ will be very high for low values of τ and negligible for higher ones. This will cause S_L to be large. If solid is exchanged at a slower rate, the average age of solid at the surface will increase, $\psi(\tau)$ will be greater for large values of τ and consequently smaller for small values, and S_L will be decreased. $\psi(\tau)$ represents the distribution of ages among the packets at the surface and is determined only by the processes causing movement of solid across and to and from the surface. $\psi(\tau)$ thus depends on the dynamics of the bed alone. S_L depends on $\psi(\tau)$ and in addition, as will be shown below, on the nature of the temperature or heat-flux distribution on the heater surface.

At present it is impossible to evaluate the stirring term S_L from the dynamic factors which determine it. However, the equations developed are still useful, for, granting the correctness of the assumptions underlying the analysis, the effect of the intrinsic thermal properties of the bed has been identified and isolated from dynamic effects. In this fact there lies an opportunity to test these assumptions experimentally; for beds that are dynamically equivalent, the observed coefficient should vary as $\sqrt{\kappa_m \rho_m c}$. If, contrary to the assumptions made, the real situation involves a gas film next to the wall as the controlling factor, changes of fluidizing gas would cause variations of the coefficient directly proportional to gas conductivity. Other possible controlling mechanisms will give other characteristic behaviors, and from the experimental evidence the admissibility of the various mechanisms may be tested.

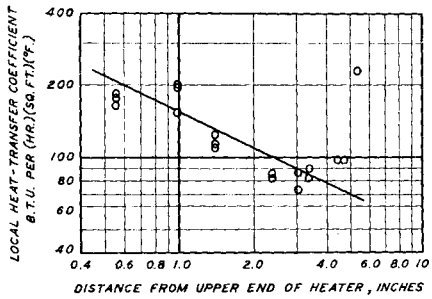

Fig. 3. Variation of the heat transfer coefficient along the vertical length of a heater. Data of Marchetti and Turner(*6*); wall heater; bed diameter: 2.75 in.; No. 11 glass beads, D_p=0.0061 in.; superficial air velocity: 0.25 ft./sec.

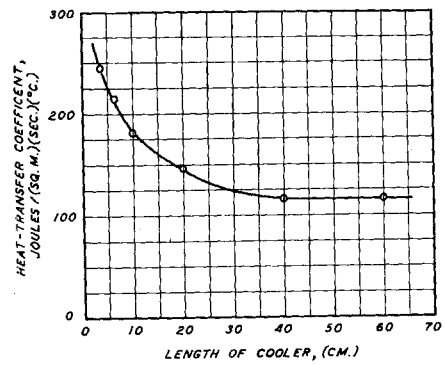

Fig. 4. Effect of cooler length on the heat transfer coefficient. Data of Van Heerden, Nobel, and Van Krevelen (*11*); wall cooler; coke fluidized with air at $V_g = 0.42$ ft./sec.

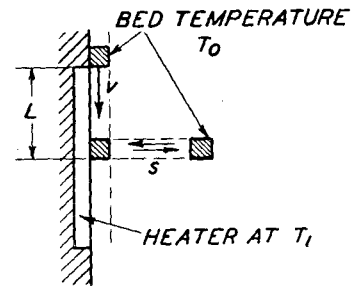

Fig. 5. Downflow of packets past a heater with superimposed side mixing from main body of the bed.

IDEALIZED BED DYNAMICS

Before the experimental checks of the effects of thermal properties are discussed, it is useful to indicate the manner in which some possible forms of bed motion might be expected to affect heat transfer. The motions which will be postulated are undoubtedly too simple to apply generally to actual fluidized beds. It is believed however that the idealized cases approximate actual conditions under special circumstances and that their study may aid in the development of qualitative ideas about the events underlying observed heat transfer phenomena.

Slug Flow of Solid Past the Surface

In a bed which is operating at very low gas rates, just above quiescence, there is not very much turbulence. The solids move up in the center and down at the walls (down also near other surfaces such as those of vertical internal heaters). The flow is not smooth but is spasmodic owing to the intermittent passage of ascending gas bubbles near by in the core of the bed. However, as one possible model of this near-quiescent system, the flow of solid downward past the wall might be assumed to be at some uniform speed v. In Figure 2, then, at a distance L from the leading edge of the heater, the age of all packets is always $\tau = L/v$, and at this position $\psi(\tau) = 0$ except for $\psi(L/v)$ which, assuming the heater to be always in contact with solid, is infinite to such an order that $\psi(L/v)\,d\tau = 1$. The stirring term S_L is then simple to evaluate; viz.

$$S_L^{1/2} = \frac{1}{\sqrt{\pi}}\int_0^\infty \tau^{-1/2}\,\psi(\tau)\,d\tau = \frac{1}{\sqrt{\pi}}(v/L)^{1/2} \quad (10)$$

and

$$h_L = \frac{1}{\sqrt{\pi}}\sqrt{\kappa_m \rho_m c}\,(v/L)^{1/2} \quad (11)$$

Equation (11) indicates that a heater in contact with such a near quiescent bed will have a heat transfer coefficient which decreases in the direction of the flow of solid along it. If there is a contributing film or surface resistance, the rate of decrease will be lessened, but if there is any degree of decrease in the local coefficient at progressively removed positions from the leading edge, this is an indication that unsteady state diffusion of heat into the flowing solids is an appreciable factor in determining the fluidized heat transfer coefficient.

Baerg, Klassen, and Gishler(*1*) made a qualitative observation of such an effect occurring with an internal heater at the center of a fluidized bed, and they concluded that there was at low gas rates a downflow of solids past the heater.

Marchetti and Turner(*6*) made rough quantitative observations of the leading-edge effect. Some of their results are shown in Figure 3, where a line of slope —0.5 fits their data fairly well. From their data, and from the known thermal properties of the solid, it is possible to estimate that the rate of solid flow v past the wall was about 1 ft./sec. This estimate is based on a modification of Equation (7) which is derived for constant-flux rather than constant-temperature heaters.

Equation (11) gives the heat-transfer coefficient at a point. The mean coefficient for the heater will be the average of the local coefficients:

$$h = \frac{1}{L}\int_0^L h_L\,dL = \frac{2}{\sqrt{\pi}}\sqrt{\kappa_m\,\rho_m\,c}\,(v/L)^{1/2} \quad (12)$$

where h is the length-mean coefficient for a surface of height L.

Dow and Jakob(*3*) have reported coefficients between bed walls and fluidized beds operated at low gas rates where an unbroken flow of solid occurred downward at the wall. They found that the observed coefficients varied as the —0.65 power of the depths of these beds. Van Heerden, Nobel and Van Krevelen(*11*) observed similar behavior when the length of cooled wall was varied and the bed depth kept constant. They concluded that the effect determined by Dow and Jakob was due to heater length, not bed depth. This is believed to be a more nearly correct interpretation.

Van Heerden et al. proposed a mechanism involving not only unsteady state transfer but also steady state conduction through a gas layer next to the heater and through a packed solid layer passing the wall. Each of these mechanisms controlled the heat transfer in turn as the solid progressed downward. Their data are shown in Figure 4. They proposed that with short heaters the solid adjacent to the wall was not heated significantly during its short contact time and that the gas layer intervening between wall and solid controlled. For longer heaters the solid began to warm significantly and the combination of gas layer resistance and heat-diffusion resistance in the solid controlled. For very long heaters, the coefficient

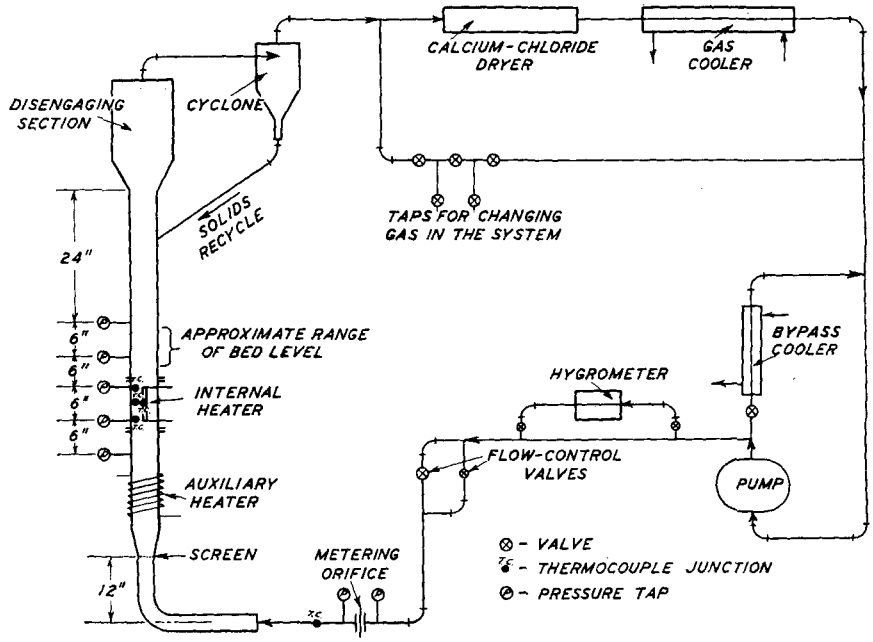

Fig. 6. Experimental fluidized system used in determining effects of gas properties on heat transfer.

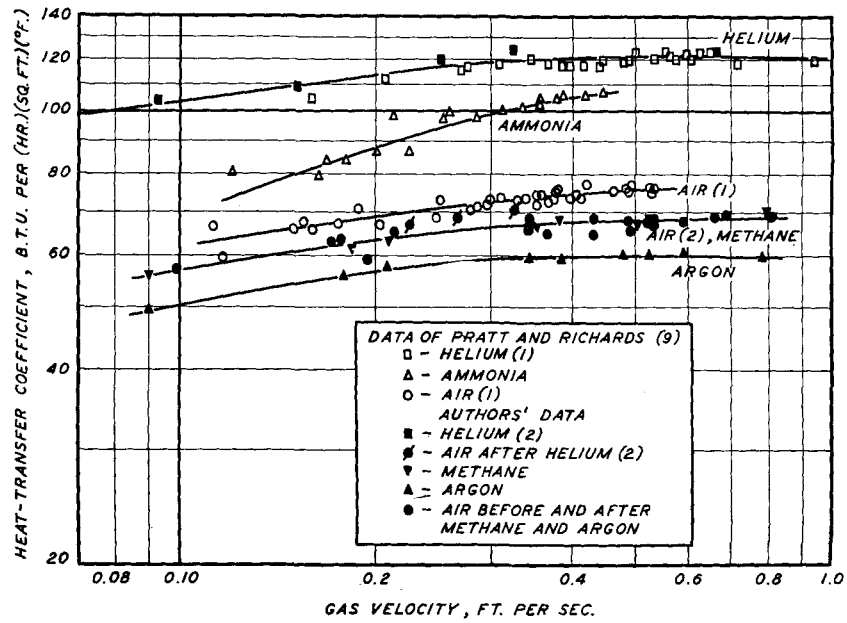

Fig. 7. Heat transfer to microspheres. Bed dimensions: Figure 6; solid properties: Table 1.

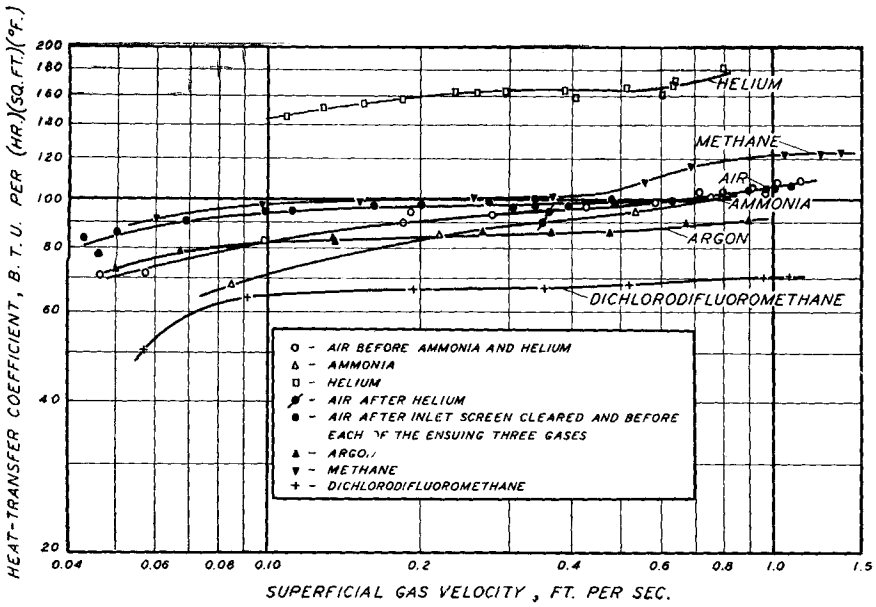

Fig. 8. Heat transfer to glass beads. Bed dimensions: Figure 6; solid properties: Table 1.

became controlled by the conduction of heat from the wall across the laminar layer of solid (now the principal resistance) to the turbulent core of the bed. Although this picture can certainly account for the heater-length effects found by these investigators, it will be shown that the data to be presented here cannot be explained by it.

From these latter data it will be seen that the principal resistance exists in the unsteady state diffusion of heat into the massed solid; independent effects of gas- and solid-layer conduction are negligible. It is believed that the length effects found by Van Heerden et al. are due mainly to variations attributable to the stirring factor S. For very short heaters of the same order of size as the length of the average pulse movement of the solid flow, S should become constant, giving a coefficient independent of length. The effect found with long heaters may be due to the fact that experimentally the heater extended into the poorly stirred solid which exists at the bottom wall of most beds, or it might be due to side mixing of solid.

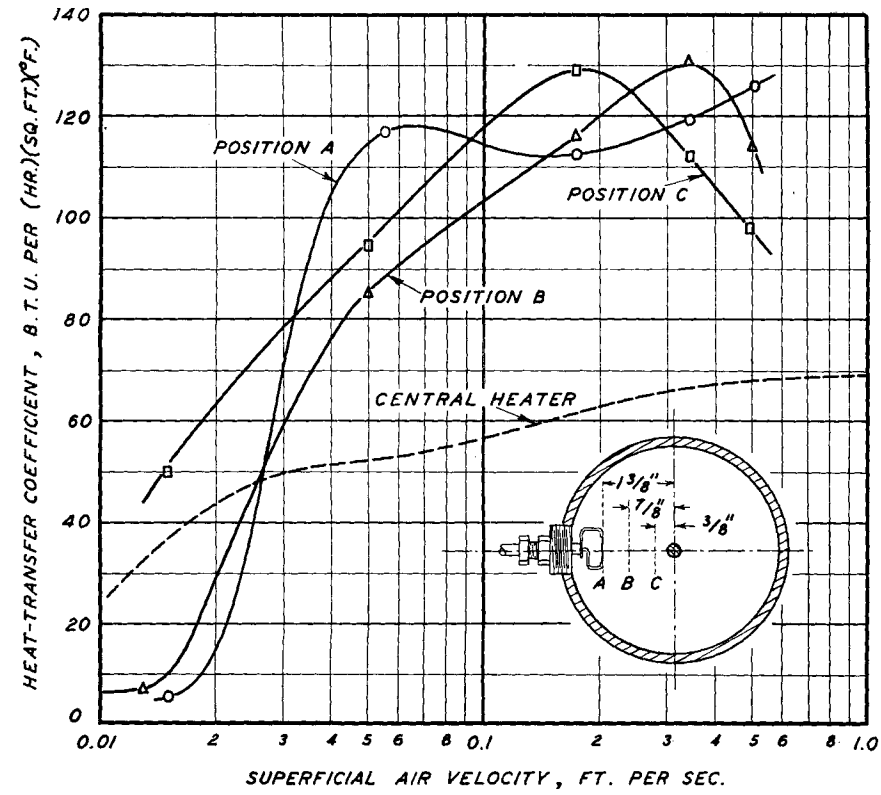

Fig. 9. Heat transfer from the heater probe to a bed of microspheres. Probe dimensions: Figure 10; solid properties: Table 1.

Side Mixing

Although slug flow of solid past the surface may in some circumstances be the primary means by which fresh solid is brought into contact with a surface, there is some evidence to indicate that with large surfaces and highly turbulent beds, sidewise transfer of solid packets to the surfaces will have an important effect on the stirring factor S.

This situation is pictured in Figure 5. Here, as before, the solid mass is flowing down past the surface, but as it passes downward some of the solid at the surface is exchanged with solid brought in sideways from the core of the bed. If s represents the average replacement of packets at the wall per unit time by means of side mixing (i.e., if $s = 0.01$ sec.$^{-1}$, during 1 sec. solid covering one hundreth of the heater area will, on the average, be exchanged by side mixing with fresh core solid), it can be shown (4) that the stirring factor S_L is

$$S_L = \left[s^{1/2} \operatorname{erf}\left(\frac{sL}{v}\right)^{\frac{1}{2}} + \left(\frac{v}{\pi L}\right)^{\frac{1}{2}} \exp\left(-\frac{sL}{v}\right)\right]^2 \qquad (13)$$

When side mixing predominates ($sL/v >> 1$), Equation (9) reduces to

$$S_L = s \qquad (14)$$

and from Equation (5)

$$h_L = \sqrt{\kappa_m \rho_m c s} \qquad (15)$$

Equation (15) is believed to represent the usual condition where transfer surfaces are large and the beds are turbulent. Values of S_L (assumed to be s) obtained in the

TABLE 1.—PROPERTIES OF SOLID MATERIALS

	No. 15 glass beads	Micro-spheres (as used)	Microspheres (as received) Not Dried	Dried*
Packed-bed density, lb./cu. ft.)				
Loose packed†	91.6	29.0	32.8	29.6
Dense packed‡	99.0	35.0	37.3	34.9
Quiescent packing**	84.3	25.0		
Particle density, by water displacement, lb/cu. ft.	153	137.7	120.3	136
Total void fraction (including internal voids)				
Loose packed	0.401	0.789	0.726	0.782
Dense packed	0.353	0.749	0.690	0.743
Quiescent packing	0.449	0.818		
Extra-particle void fraction¶				
Dense packed	0.35	0.29		
Quiescent packing	0.45	0.49_3		
True particle density, lb./cu. ft.	153	49.3¶		
Average particle diameter, in.	0.0032_5	0.0027		

*Oven-dried at 220°F.
†After being gently poured into container.
‡After prolonged tapping of container.
**From pressure gradient in fluidized condition, extrapolated to quiescence.
¶From analysis of thermal conductivity data. Assumed to include internal voids of individual particles as parts of the particles.

present experiments and believed to represent a typical order of magnitude were about 4 and 10 sec.$^{-1}$ for fluidization of the glass beads and the microspheres respectively.

It should be noted that all equations developed here are for constant-temperature surfaces. If constant-flux (electrically heated) surfaces are used, the constant $1/\sqrt{\pi}$, in Equation (2) becomes $\sqrt{\pi}/2$ and a different definition of the average coefficient is required. The constant-flux analogue of Equation (13) is

$$S_L = \left[\frac{s^{1/2}}{\operatorname{erf}\left(\frac{sL}{v}\right)^{\frac{1}{2}}}\right]^2 \quad (16)$$

and for $s \to 0$ Equation (16) can be shown to yield the analogue of Equation (10), viz.,

$$S_L^{1/2} = \frac{\sqrt{\pi}}{2}(v/L)^{1/2} = \frac{1.571}{\sqrt{\pi}}(v/L)^{1/2} \quad (17)$$

It can be seen that when laminar flow past the surface predominates, an electrical heater will give local coefficients 57% greater than would an isothermal heater. Equations (14) and (15), however, apply to both types of heaters when side mixing predominates.

It is not expected that the equations developed above can be used at present to predict heat transfer with assurance. For this purpose dependable means of predicting solid motion are needed. Experimentally the equations may serve this end by allowing determination of solid motion by means of heat transfer measurements. The above-mentioned development was carried out chiefly to allow a qualitative understanding of the mechanism here proposed.

TABLE 2.—MEASURED CONDUCTIVITIES OF BEDS

Interstitial gas	Gas conductivity B.t.u./(hr.)(ft.)(°F.)	Conductivity of dense bed, B.t.u./(hr.)(ft.)(°F.)	Estimated quiescent conductivity, B.t.u./(hr.)(ft.)(°F.)
Solid: glass beads; bed density: 99.0 lb./cu. ft.			
Air	0.0149	0.0895	0.0620
	0.0148	0.0938	0.0650
	0.0149	0.0893	0.0619
	0.0149	0.0930	0.0645
	0.0149	0.0923	0.0639
Helium	0.0823	0.2188	0.1760
	0.0823	0.2295	0.1850
Methane	0.0188	0.1109	0.0783
Ammonia	0.0140	0.0867	0.0597
Argon	0.0101	0.0687	0.0462
Freon-12	0.00597	0.0484	0.0314
	0.00594	0.0506	0.0328
Solid: microspheres; bed density: 35.0 lb./cu. ft.			
Air	0.0155	0.0505	0.0328
	0.0155	0.0515	0.0335
Helium	0.0839	0.0989	0.0928
	0.0840	0.0980	0.0921
Methane	0.0201	0.0570	0.0390
Ammonia	0.0132	0.0476	0.0300
Argon	0.0104	0.0422	0.0254

The estimated conductivities of the solid particles used in fitting the data to the Schumann-Voss relation (Figure 12) were glass beads, 0.7 B.t.u./(hr.)(ft.)(°F.); microspheres, 0.106 B.t.u./(hr.)(ft.)(°F.). These two conductivities were not measured directly and should be regarded as approximate.

TEST OF THE MECHANISM

Because solids motion cannot be independently determined, it might appear impossible to test the proposed mechanism. However, this is only partly true. The tests that will be presented are based on the assumption that if the heater-bed configuration is the same, the bed motions characterizing S will be nearly the same for a given solid when fluidized at the same gas rate, independent of the physical properties (i.e., viscosity and density) of the gas. This assumption cannot be catagorically proved; nevertheless, on the basis of it a remarkable consistency can be shown to exist among the heat transfer measurements made, a consistency that would be very unusual if the assumption were not a reasonable one.

Granting that bed motion is nearly independent of gas viscosity and density, consideration of the equations developed in the last section shows that the heat transfer coefficient should vary as the square root of the packet conductivity (i.e., the conductivity of the quiescent bed) so long as packet density and heat capacity remain constant. Mechanisms depending on a gas- or solid-film model would, on the other hand, yield variations of the coefficient directly with gas or packet conductivities. For this reason, experiments were carried out in which heat transfer coefficients were measured in beds of solids fluidized with several different gases. The conductivities of beds of these solids were also measured.

EXPERIMENTAL PROCEDURE

The bed in which heat transfer coefficients were measured is shown in Figure 6. The fluidization section was a 4-in. I.D. tube and the heater was a 6-in. section of ¼-in. stainless steel tubing. The heater was supported coaxially in the bed by copper rods at either end. Heat was supplied by passing current through the length of the tube wall, the heat output being obtained from the measured cur-

TABLE 3.—SUMMARY OF EFFECTS OF VARIABLES ON THE STIRRING FACTOR, S

Variable	Exponent in Eq. (20)	Experimental values of exponents	Reference
Particle diameter, D_p	a_1	-0.6, -1.2	1, 7
Quiescent density, ρ_m	a_2	-1.1	Present
Gas viscosity, μ_g	a_3	Small	Present
Gas velocity, V_g	a_4	Widely different effects noted, power function inadequate	
Gas density, ρ_g	a_5	$-0.2 < a_5 < 0.2$	Present
Heater length, L	a_6	$-1.0\left(\frac{sL}{v}\text{ small}\right)$ to $0\left(\frac{sL}{v}\text{ large}\right)$	Present
Solids concentration, α_s	a_7	0(low V_g), -1.0($V_g > 1.0$ ft./sec.)	7

Other factors include: 1. Size and geometry of bed and heater
2. Type of heater, constant-temperarure, constant flux, or other
3. Particle roughness
4. Adsorption of vapors on particle surfaces

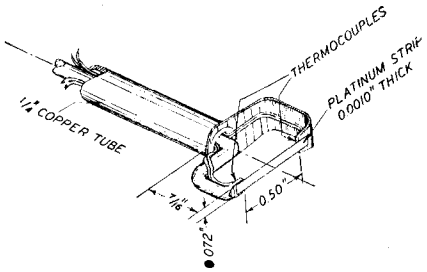

Fig. 10. Isometric sketch of the heater probe.

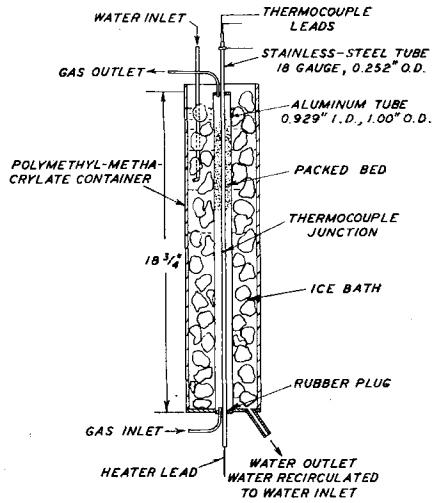

Fig. 11. Apparatus for determination of thermal conductivities of packed solids.

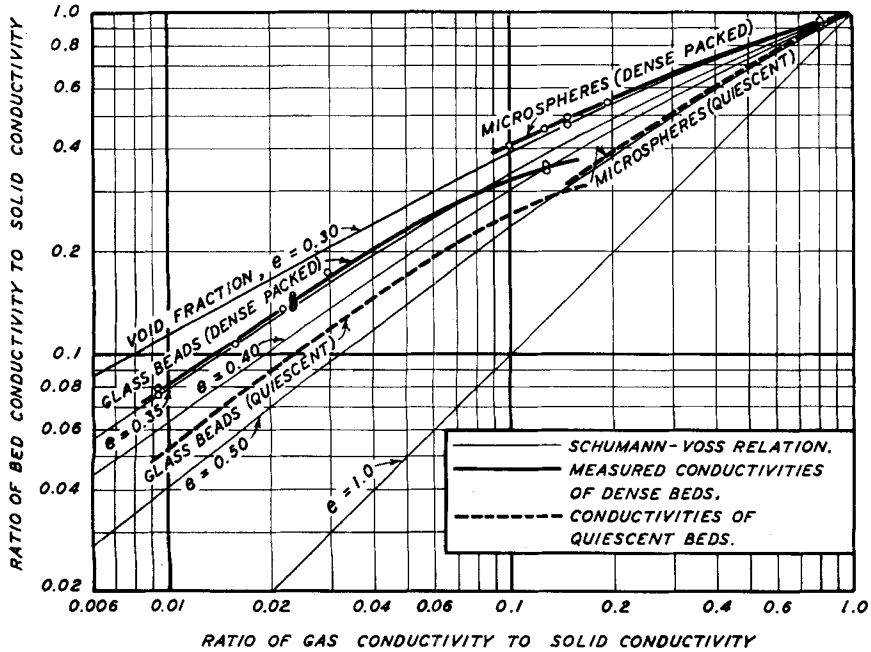

Fig. 12. Conductivities of beds of packed solids. Measured conductivities are shown correlated with Schumann-Voss relation. Quiescent conductivities were obtained from plot by allowing for change of void fraction.

rent and known resistance of the tube. Bed and heater temperatures were measured thermoelectrically, the heater thermocouple being inside the tube at the middle but electrically insulated from it.

During operation, gas was recycled to the bed through a totally closed system which included a cooling section and calcium chloride drier. Table 1 gives properties of the two solid types. The quiescent velocities for these solids, as detected by the onset of bed manometer fluctuation, were small compared with the fluidizing velocities used. Quiescent densities of the fluidizing solids were estimated from the solids concentrations obtained at very low gas velocities. These densities, which are given in Table 1, were, within experimental precision, independent of the gas used.

The heat transfer coefficients obtained are shown in Figures 7 and 8. In the obtaining of these coefficients the temperature difference between heater and bed was given by bucking thermocouples. Fluctuations of the temperature difference of up to $\pm 10\%$ were observed over short intervals of time even though the heating current was constant. Each of the coefficients given is based on the average of about thirty readings of the temperature difference taken over a period of 10 to 15 min.

Some supplementary data obtained with a very small heater probe inserted various distances into the air-microsphere bed are shown in Figure 9. The probe (Figure 10) was a strip of platinum ribbon ½-in. long, 0.072 in. wide, 0.0010 in. thick, its major surface being used in a vertical plane with the long dimension horizontal. The ribbon was heated by direct current, and from its resistance the average temperature was obtained. From this temperature and the current, coefficients were calculated, allowance being made for conduction losses at the ends and the variation of temperature along the length of the ribbon.

The conductivities of the packed solids in the presence of the various gases were measured in a cylindrical apparatus shown in Figure 11. Although the conductivities of quiescent packing were desired under the measurement conditions, the solids were dense packed. The correlations of Schumann and Voss(*10*) were used to adjust the measured values for the difference between these two packings. Both the measured and the adjusted values are given in Table 2, and these data are shown in Figure 12, superimposed on the Schumann-Voss correlation.

RESULTS

1. Probably the most significant result appears when the heat transfer coefficients obtained with the various gases are compared with

the quiescent conductivities of the beds. This has been done in Figures 13 and 14, and it can be seen that for the most part the heat transfer coefficient appears to vary as the 0.52-0.55 power of the quiescent conductivity for a given solid and given gas velocity. The major deviation from this rule occurs in the case of the coefficients obtained with the ammonia-microsphere system, for which the coefficients are 30 to 40% too high. This discrepancy has a reasonable and revealing explanation, which will be discussed below. Except for this one case, the data are consistent, the deviations being easily attributable to experimental error or to small systematic effects of gas viscosity and density on the bed dynamics.

The consistency of the data in these two figures constitutes major evidence for the correctness of the proposed heat transfer mechanism. The effect of quiescent conductivity is very closely the square-root variation expected. If, on the other hand, heat transfer had been controlled by conduction through a laminar layer of solid, the expected variation would have been as the first power of quiescent conductivity. If a gas film had been the controlling factor, the variation should have been as the first power of gas conductivity, and, since, with the gas-solid systems employed, quiescent bed conductivity varied as about the 2/3 power of gas conductivity (*see* Figure 12), the slopes in Figures 13 and 14 would have been approximately $1 \div 2/3 = 1.5$.

It is concluded that the packet mechanism is a reasonable picture of the heat-transfer process in fluidized beds.

2. The measured coefficients varied only slightly with gas velocity. Such a lack of important influence of gas velocity has been previously reported by some investigators. Others have found variations ranging from nearly direct to inverse. The reason for this variety of results is not clear and is certainly deserving of further attention.

In this respect it should be noted that the heat transfer coefficients obtained with the small heater probe (Figure 9) display a variety of effects of gas velocity. The interpretation of these probe data is somewhat speculative, but they seem to indicate that fluidization at the lowest velocities occurred only at the center of the bed, i.e., that there was "bubble channeling." As the gas velocity was increased, fluidization quickly extended to the rest of the bed. It is believed that the drop-off of the coefficients near the center of the bed at the higher velocities resulted from the tendency of gas bubbles to congregate there, leaving the small probe frequently out of contact with solid material. Apparently in the vicinity of vertical surfaces (the wall and the central heater) the solid concentration remained high. It can be concluded that the bed was not, in general, homogeneous, that solid preferentially sought the vicinity of large surfaces while the gas bubbles crowded into the spaces between and away from such surfaces.

That much higher coefficients were obtained with the heater probe is believed attributable to the small size of the probe compared with the central heater.

3. There was no noticeable independent effect of solids concentration on heat transfer. In some cases different gases gave significantly different solids concentrations at the same gas rate. These differences had no noticeable correlation with heat transfer nor did they correlate systematically with

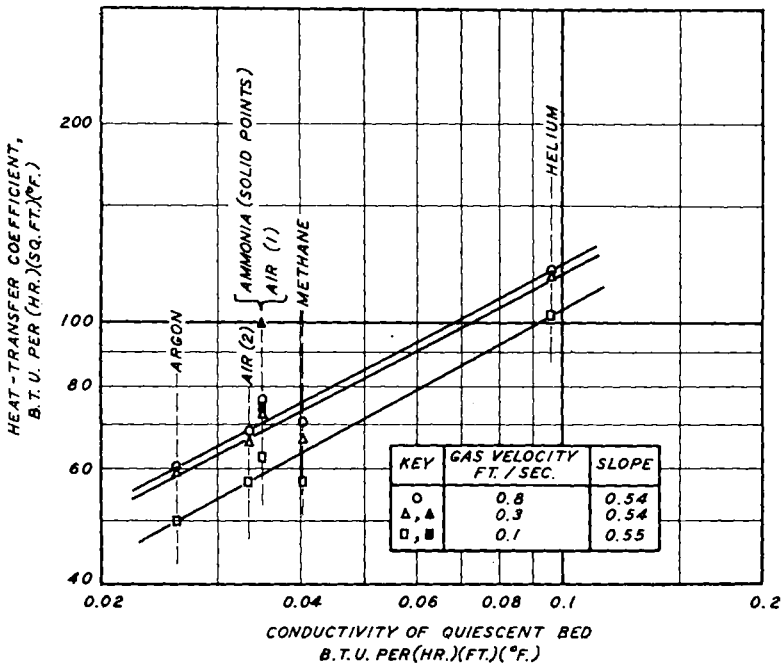

Fig. 13. Microspheres: the heat transfer coefficient as a function of quiescent-bed conductivity.

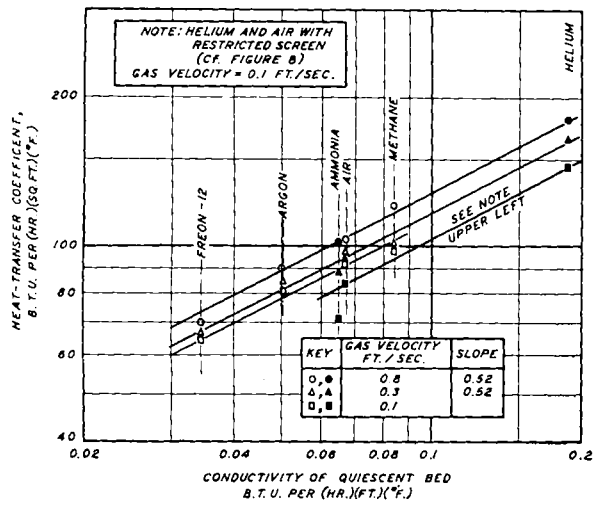

Fig. 14. Glass beads: the heat transfer coefficient as a function of quiescent-bed conductivity.

the viscosities and densities of the gases.

4. Increasing the gas pressure from 1.0 to 1.3 atm. had no noticeable effect on heat transfer when the superficial velocity was maintained constant.

5. Comparison of the coefficients obtained with microspheres with those obtained with glass beads indicated that density, as characterized by quiescent density, had almost no effect on the heat transfer coefficient, i.e., that S varied as the —1.1 power of quiescent density, thereby nearly canceling the effect of quiescent density indicated by ρ_m in Equations (1) to (15). This result would seem to indicate that lighter particles move faster at equal fluidization velocities.

6. The ammonia - microsphere system behaved paradoxically. It has already been noted that with this system the heat transfer coefficients were higher than expected. When ammonia was first introduced into the microsphere bed, a large heat evolution was noted, and it was concluded that adsorption of ammonia was occurring on the porous microspheres. This conclusion was substantiated by the fact that the microspheres, which displayed a quiescent density with other gases before and after their fluidization with ammonia of 25.0 lb./cu.ft., had a quiescent density of about 29.8 lb./cu.ft. in the presence of ammonia. Because, as stated in section 5 above, heat transfer is nearly independent of quiescent density, the increased weight of the particles could not be the main source of the 30 to 40% excess in the ammonia-microsphere coefficients.

However, the heat capacity of liquid ammonia is high, viz., 1.163 B.t.u./(lb.)(°F.). The microspheres themselves have a heat capacity of about 0.16 B.t.u./(lb.)(°F.). Assuming that the adsorbed ammonia behaves as the liquid, the saturated microspheres would have a heat capacity of

$[(0.16)\ (25.0) + 1.163\ (4.8)]/29.8 = 0.32$ B.t.u./(lb.)(°F.)

From Equation (15) it would be expected that the saturated microspheres would display coefficients higher by an amount equal to the ratio of the square roots of the heat capacities. Since the ratio of the heat capacities is $0.32/0.16 = 2$, and since $\sqrt{2} = 1.41$, a 40% increase can be adequately explained. This only explains in part the misbehavior of the ammonia-microsphere system, for at lower gas velocities, below 0.2 ft./sec., the coefficients obtained were only about 30% too high. In Figure 8 it will be noted that for the ammonia–glass bead system there is a similar drop-off of the coefficients at low gas velocity. The glass beads were nonporous and gave no gravimetric evidence of ammonia adsorption; however, it appears likely that some of the gas condensed on the glass surfaces. Such condensation has been found by other investigators to cause bed particles to stick together and to increase the probability of channeling.

DISCUSSION

Effect of Particle Size

The present investigation included no direct determination of the independent effect of particle size. Other investigators have universally found that with a given bed and heater and the same gas and solid type the heat transfer coefficient increases as the average particle size diminishes. Mickley and Trilling (*7*) found that $h \propto D_p^{-0.6}$, and Baerg et al. (*1*) found that $h \propto D_p^{-0.3}$. The usual interpretation has been that the effect is due to the reduction in thickness of a gas film which offers appreciable resistance to the conduction of heat between heater and solid particles. But the present work shows that no such appreciable gas-film resistance is present.

Here the alternative proposal is made that the particle-size effect is one of bed motion, that beds of smaller particles circulate fresh solid to contacting walls more rapidly at a given gas velocity. In terms of Equations (1) to (16), this means that the stirring factor S is a decreasing function of particle diameter.

Effects of Solids Concentration

As has been mentioned, no independent effect of solids concentration (the ratio of apparent bed density to quiescent density) was noted in the present investigation. However, Mickley and Trilling, employing a higher range of gas velocities (1 to 6 ft./sec.), found that the heat transfer coefficient varied as the 0.48 power of solids concentration. This effect implies that S, the stirring factor, varies as the 0.96 power of solids concentration at high gas velocities.

One possible (but not a unique) interpretation of this relationship is that, when it applies, the heated surface is only partially covered with solid and that, more precisely, the average fraction of the heated surface in contact with dense-phase material is directly proportional to the solids concentration. Meanwhile the rate of formation of fresh area of contact is independent of solids concentration.

Actually, this seems to be a reasonable picture of a slugging bed, but it is to be recognized that, at the higher gas velocities, mechanisms other than the one here proposed may be important in determining the total resistance of the bed to heat transfer.

Mass Transfer to Fluidized Beds

Recently Van Heerden, Nobel, and Van Krevelen (*11*) investigated the transfer of naphthalene to fluidized beds of coke and Devarda's alloy. A ring of naphthalene 6 cm. high was coated on the inner wall of the bed, and with air blowing through the bed at a superficial velocity of 0.42 ft./sec. the mass-transfer coefficients were determined. It was noted that with both types of solid the value of the coefficient declined rapidly with increasing temperature. The coke bed, for instance, yielded a coefficient, k_g, of 9.3 cm./sec. at 5.1°C., whereas at 33.0°C. k_g was 1.45 cm./sec. Heat transfer coefficients were also determined to a heat transfer ring, also 6 cm. high, placed in the beds in the same place as the naphthalene surface. The air rate was the same as before (0.42 ft./sec.). It is illuminating to study these data in the light of the picture of the fluidization mechanism that has been developed here and, especially, to determine what relalationship may exist between the processes of mass and heat transfer.

It will be assumed that mass transfer occurs in a manner completely analogous to the mechanism already developed for heat transfer. On the basis of this assumption, it is easily shown that the mass transfer analogue of Equation (1) is

$$N_m = \frac{A_m}{\sqrt{\pi}} \sqrt{\mathbf{D}_m \rho_m \left(\frac{C_M}{y_s}\right)}\ \tau^{-1/2} (y_s - y_e) \qquad (18)$$

where

N_m = rate of mass transfer, g./sec.
A_m = area of transfer surface, sq. cm.

$\mathbf{D}_m$ = diffusion coefficient of the transferring component through the dense phase, sq. cm./sec.

ρ_m = density of the dense phase, g./cc.

C_M = mass-capacity coefficient of the adsorbent (*see* below for full definition), dimensionless

τ = age or time of contact of the adsorbent packet with the surface, sec.

y_s = saturation concentration of the diffusing component in the vapor phase when in equilibrium with the solid, g./cc.

y_e = concentration of the volatile material in the gas phase of the main body of the bed, g./cc.

The mass-capacity coefficient C_M needs fuller explanation. The "mass capacity," C_M/y_s, is the analogue of the heat capacity and represents the mass of additional adsorbate which will be retained by unit mass of the adsorbent following a unit increase in the concentration, y_e, of adsorbate in the vapor phase; that is, if at constant, temperature N_A represents the grams of adsorbate retained on 1 g. of adsorbent, then

$$dN_A = \left(\frac{C_M}{y_e}\right) dy_e \qquad (19)$$

The value of C_M can be determined from the adsorption isotherms of the components involved. It should be noted that C_M is not independent of the vapor concentration, y_e. For the present purpose some value typical of the range of concentration from y_e to y_s is to be selected. Referring to Figure 15, which shows two adsorption isotherms for naphthalene and coke(*11*), the value of C_M is estimated from the slope of the dashed line as 0.000245 at 3.5°C. and as 0.000274 at 17.7°C. From Figure 15 the value of C_M for Devarda's alloy and naphthalene will be taken as 0.0000202 at 0.7°C. It is also to be noted that although C_M, the mass-capacity coefficient, is relatively insensitive to temperature in the present case of physical adsorption, the mass-capacity C_M/y_s decreases markedly with increasing values of the saturation concentration, y_s, and thus with increasing temperature.

From Equation (18), by direct analogy to the development of Equation (9) from Equation (1), it may be shown that

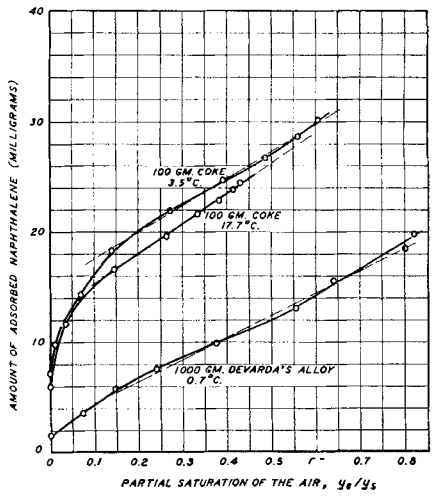

Fig. 15. Adsorption isotherms for naphthalene on coke and Devarda's alloy. Data of Van Heerden, Nobel, and Van Krevelen(*11*).

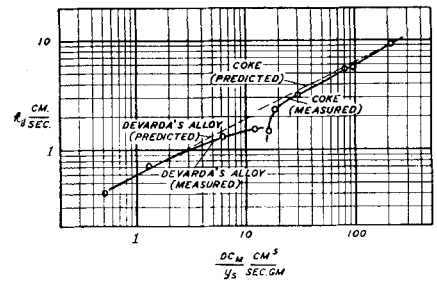

Fig. 16. Comparison of experimental mass transfer coefficients with values predicted from heat transfer coefficients. Data of Van Heerden, Nobel, and Van Krevelen(*11*).

$$k_g = \sqrt{\mathbf{D}_m \rho_m \left(\frac{C_M}{y_s}\right) S} \qquad (20)$$

where k_g is the average mass transfer coefficient between bed and wall (cm./sec.)

If reasonable values can be estimated for the mass transfer and thermal properties of the beds, it should be possible to evaluate the "stirring term," S, from the measured heat transfer coefficient and to use this value in Equation (20) to obtain the mass transfer coefficient. The estimated mass transfer coefficients may then be compared with those obtained experimentally by Van Heerden, Nobel and Van Krevelen.

Exact data are not available for the properties of quiescent coke or Devarda's alloy, and some approximation is necessary.

By use of the data of Dow and Jakob(*3*) for fluidized coke, the quiescent void fraction is estimated as, $\varepsilon_m = 0.634$. Since coke is a relatively high-conductivity solid, it is estimated, with the aid of reference *10*, that $\kappa_m = 2.7$ $\kappa_g = 2.7 \times 0.016 = 0.043$ B.t.u./(hr.)(ft.)(°F.). The heat capacity of coke is taken as $c = 0.223$ B.t.u./(lb.)(°F.). The quiescent density is taken as 44.4 lb./cu.ft. or 0.713 g./cc.

From Equation (9)

$$S = \frac{h^2}{\kappa_m \rho_m c} \qquad (21)$$

Van Heerden et al. obtained a heat transfer coefficient with coke of 230 Joules/(sq.meter)(°C.)(sec.) or 40.25 B.t.u./(hr.)(sq. ft.)(°F.). By means of Equation (21) a value of $S = 1.056$ sec.$^{-1}$ is calculated.

Data are available for the diffusion coefficient of naphthalene in air, and if it is assumed that there is relatively little diffusion through the coke particles, a relation developed by Maxwell(*5*) allows the estimation of the over-all diffusion coefficient of napthalene through a bed of void fraction, $\varepsilon_m = 0.634$. This gives $\mathbf{D}_m = 0.535\ \mathbf{D}$ where $\mathbf{D}$ is the diffusivity of naphthalene into air with no obstruction present in the diffusion path. Substituting the necessary values into Equation (20) (shifting to c.g.s. system of units) gives

$$k_g = \sqrt{(0.535)\,\mathbf{D}\,(0.713)\,\frac{C_M}{y_s}\,(1.056)}$$

$$= 0.635\sqrt{\frac{\mathbf{D}C_M}{y_s}}$$

Figure 16 shows this relationship plotted as a dashed line with the data of Van Heerden et al. superimposed. The data for Devarda's alloy were treated similarly and are also plotted.

It is to be noted that notwithstanding the possible imprecision of some of the estimated bed properties used in the calculations, the magnitude of the experimental mass-transfer coefficients is fairly well predicted. Perhaps even more significant is that a decrease in the coefficient obtained with increasing temperature is predicted in fair accordance with the observed behavior. It is concluded that this decrease in coefficient with increasing temperature is due to the increase in vapor pressure of the adsorbate and consequent reduction in the "mass capacity" of the adsorbent.

The ability to correlate mass and heat transfer seems to offer

further confirmation for the proposed transfer mechanism.

CONCLUSION

The results of the present investigation indicate that the principal resistance to the transfer of heat or mass from surfaces to dense fluidized beds exists in the layers of solid particles nearest the surface. The rate of transfer appears to be controlled by the unsteady state diffusion of heat or mass into this layer and by the rate of replacement of parts of this layer with solid from the bed core. There is no evidence of a steady state film of gas or solid offering significant resistance.

The functional relationship of the heat-transfer coefficient to other bed properties is adequately comprehended by equations of the form

$$h = \sqrt{\kappa_m \rho_m c S} \qquad (9)$$

where S, the stirring factor, accounts for the type and degree of bed motion and also may be affected by the type, size, and position of the heat source. At the present time too little is known about bed motion in the vicinity of surfaces to relate S analytically to the parameters suspected of determining bed motion. It is believed to be a function of many variables; thus

$$S = \phi_1 (D_p, \rho_m, \mu_g, V_g, \rho_g, L, \alpha_s, \text{and others}) \qquad (22)$$

Some of the functional variations have been determined both here and by other investigators. Thus if the foregoing equation could be represented as a product of powers of the factors, i.e.,

$$S = D_p^{a_1} \cdot \rho_m^{a_2} \cdot \mu_g^{a_3} \cdot V_g^{a_4} \cdot \rho_g^{a_5} \cdot L_g^{a_6} \cdot \alpha_s^{a_7} \cdot \phi_2 \text{ (other factors)} \qquad (23)$$

the values for the exponents that have been mentioned in the present paper are summarized in Table 3.

More work on the mechanics of fluidized beds is needed if it is to be possible to predict heat transfer coefficients adequately. It is recommended that data be reduced to the form

$$S = \frac{h^2}{\kappa_m \rho_m c} \qquad (21)$$

and that the correlation of S with operating variables and the characteristics of the solids be made.

It should be noted that if trustworthy data are available for a bed-heater system fluidized with one gas, the present findings make possible the prediction with fair reliability of coefficients with another gas.

However, until heat transfer data more comprehensive than those presently available appear, the use of stirring-factor correlations based on such data must be treated with caution when applied to uninvestigated ranges of the many variables.

NOTATION

A = area of heat transfer surface, sq.ft.

A_m = area of packet in contact with heat transfer surface, sq.ft.

a_1-a_7 = exponents in Equation (23)

C_M = mass-capacity coefficient of solid adsorbent, dimensionless

c = heat capacity of fluidized solid, B.t.u./(lb.)(°F.)

$\mathbf{D}$ = diffusion coefficient of transferring component through fluidizing gas, sq.cm./sec.

$\mathbf{D}_m$ = diffusion coefficient of transferring component through fluidized solid-gas mixture, sq.cm./sec.

D_p = average diameter of the fluidized particles, ft.

erf = error function

exp = exponential function

h = coefficient of heat transfer from surface to bed (time and local-area average), B.t.u./(hr.)(sq.ft.)(°F.)

h_i = instantaneous heat transfer coefficient, B.t.u./(hr.)(sq.ft.)(°F.)

h_L = local time-average heat transfer coefficient, B.t.u./(hr.)(sq.ft.)(°F.)

k_g = coefficient of mass transfer from surface to bed (time and local-area average), cm./sec.

L = length of heater from upper edge, ft.

N_A = amount of component adsorbed per unit of adsorbent, g./g.

N_m = instantaneous mass transfer rate between bed and surface, g./sec.

q_m = instantaneous heat transfer rate between bed and surface, B.t.u./hr.

S = area-mean stirring factor, hr.$^{-1}$

S_L = local stirring factor $= 1/\pi (\int_0^\infty \tau^{-\frac{1}{2}} \psi(\tau)\, d\tau)^2$ (hr.$^{-1}$)

s = fraction of heater-surface area contacted by fresh packets from the main body of the bed per unit time, sq.ft./(hr.)sq.ft.

T = temperature, °F.

t = time, hr.

V_g = superficial fluidizing-gas velocity, ft./sec.

v = average downward velocity of solid past a vertical surface, ft./hr.

y_e = concentration of component in gas-phase, g./cc.

y_s = concentration of component in gas phase in equilibrium with adsorbent, g./cc.

α_s = solids concentration, ratio of bed density to quiescent density

ε_m = void fraction of quiescent bed

κ_g = thermal conductivity of fluidizing gas, B.t.u./(hr.)(°F.)(ft.)

κ_m = thermal conductivity of quiescent bed, B.t.u./(hr.)(°F.)(ft.)

μ_g = viscosity of fluidizing gas, centipoises

ρ_g = density of fluidizing gas, lb./cu.ft.

ρ_m = density of quiescent solid, lb./cu.ft.

τ = packet age, i.e., time during which packet has been in contact with surface, hr.

$\psi(\tau)$ = frequency of occurrence, at a point on the heater surface, of packets of age τ, hr.$^{-1}$

$\pi = 3.14159$

$\phi(x)$ = function of x

LITERATURE CITED

1. Baerg, A., J. Klassen, and P. E. Gishler, *Can. J. Research*, **28F**, 287 (1950).
2. Bauer, W. C., Sc.D. thesis, Mass. Inst. Technol. (1949).
3. Dow, W. M., and M. Jakob, *Chem. Eng. Progr.*, **47**, 637 (1951).
4. Fairbanks, D. F., Sc.D. thesis, Mass. Inst. Technol. (1953).
5. Jakob, M, "Heat Transfer," p. 85, John Wiley and Sons, Inc., New York (1949).
6. Marchetti, E. J., and R. A. Turner, S.B. thesis, Mass. Inst. Technol. (1951).
7. Mickley, H. S., and C. A. Trilling, *Ind. Eng. Chem.*, **41**, 1135 (1949).
8. Nicholson, E. W., J. E. Moise, and R. L. Hardy, *Ind. Eng. Chem.*, **40**, 2033 (1948).
9. Pratt, S. L., Jr., and R. L. Richards, Jr., S. M. thesis, Mass. Inst. Technol. (1951).
10. Schumann, T. E. W., and V. Voss, *Fuel*, **13**, 249 (1934).
11. Van Heerden, C., P. Nobel, and D. W. Van Krevelen, *Ind. Eng. Chem.*, **45**, 1237 (1953).